

Towards a median signal detector through the total Bregman divergence and its robust analysis

Yusuke Ono* and Linyu Peng†

*Department of Mechanical Engineering, Keio University,
Yokohama 223-8522, Japan*

May 10, 2022

Abstract

A novel family of geometric signal detectors are proposed through medians of the total Bregman divergence (TBD), which are shown advantageous over the conventional methods and their mean counterparts. By interpreting the observation data as Hermitian positive-definite (HPD) matrices, their mean or median play an essential role in signal detection. As is difficult to be solved analytically, we propose numerical solutions through Riemannian gradient descent algorithms or fixed-point algorithms.

Beside detection performance, robustness of a detector to outliers is also of vital importance, which can often be analyzed via the influence functions. Introducing an orthogonal basis for Hermitian matrices, we are able to compute the corresponding influence functions analytically and exactly by solving a linear system, which is transformed from the governing matrix equation. Numerical simulations show that the TBD medians are more robust than their mean counterparts.

Keywords: Geometric median, matrix-CFAR, robust analysis, nonhomogeneous clutter

1 Introduction

In target detection, the constant false alarm rate (CFAR) is a well-known and conventionally used clutter suppression method [29]. A popular CFAR is based on Fourier transform and makes use of the Doppler spectral density to distinguish targets from clutter. However, this method is rather weak for short waveform of dense and nonhomogeneous clutter. One of the popular statistical methods for discriminating between the target signal from clutter is to estimate the covariance matrix and test the likelihood ratio. There has been a well-known method for estimating the clutter covariance matrix, namely, the sample covariance matrix (SCM) using the maximum likelihood estimation [15], but this method performs well only when enough number of signals is independent and identically distributed [28]. In order to reduce the number of required observation data for achieving efficient detection performance within nonhomogeneous clutter, various knowledge-based methods using *a priori* information were proposed [10, 23, 24, 32, 34]. In [2, 6], the Bayesian methods were leveraged to estimate the covariance matrix. In practice, it is hard to accurately capture the statistical information of clutter in advance which can be range-dependent and non-stationary and the observation data is usually contaminated. Insufficient knowledge of clutter environment can lead to the detection performance degradation.

Recently, the matrix-CFAR, which needs no *a priori* information but makes use of the covariance matrix of the signals, was proposed and developed [3, 4]. It is based on the fact that the covariance matrix that represents the correlation of complex signals is Hermitian positive-definite (HPD). It was applied to target detection [35] and drone detection [7]. Its advantages have been demonstrated in detection of high frequency X-band radar clutter [22], Burg estimation of radar scatter matrices [12], monitoring of wake eddy turbulence [5], etc. In recent years, the matrix-CFAR with respect to various divergence functions has been proposed, and its detection performance and robustness to outliers were shown better compared with that of the geodesic distance associated to the affine-invariant Riemannian metric (AIRM) [17–19].

*E-mail: yuu555yuu@keio.jp

†Corresponding author. E-mail: l.peng@mech.keio.ac.jp

In this study, the total Bregman divergence (TBD) defined in HPD manifolds is applied to signal detection. In particular, to improve the robustness of the matrix-CFAR, we extend the previous study [20] on TBD means to medians as median detectors are often more robust to outliers than the mean counterparts. Main contributions of the current paper are outlined as follows.

- (1) We define the TBD medians associated with the total square loss (TSL), the total log-determinant (TLD) divergence and the total von-Neumann (TVN) divergence, and investigate their detection performance compared with the TBD means, the Riemannian distance (RD) mean and median associated to the AIRM as well as the generalized likelihood ratio test (GLRT) detector. Medians are often difficult to be calculated analytically; instead, we introduce fixed-point algorithms or Riemannian gradient descent algorithms to solve them numerically.
- (2) Influence functions are often used to describe the robustness of a detector about outliers. As noticed in [20], the matrix equations for influence functions are not commonly seen in matrix theory and to solve them directly can be very challenging. By defining an orthogonal basis for Hermitian matrix spaces with the induced Frobenius metric, we transform those matrix equations to linear systems, which can immediately (at least in principle) be solved exactly. This methodology allows us to precisely capture the robustness of all means and medians discussed in the current paper.

The structure of this paper is as follows. Theory of the matrix-CFAR is summarized in Section 2. In Section 3, after briefly reviewing the geometry of HPD equipped with the AIRM, we introduce Riemannian gradient descent algorithms for solving the corresponding RD mean and median. Riemannian gradient, also called natural gradient, assigns the steepest direction in Riemannian manifolds. Furthermore, the TBD medians are defined and solved numerically through the fixed-point algorithms. Numerical detection performance is conducted in Section 4 by comparing the RD mean and median, the TBD means and medians, and the conventional GLRT. In Section 5, an orthogonal basis for Hermitian matrices is defined and applied to the computation of influence functions, allowing us to accurately illustrate robustness of all means and medians. We conclude and address several lines of potential future researches finally in Section 6.

2 Formulation of the matrix-CFAR

In this section, the method of matrix-CFAR will be recalled. Assume that the observation data are collected from N stationary channels and consider a detection problem concerning a moving target under the nonhomogeneous clutter environment. The problem of detection will be modeled as a binary hypothesis testing. In this testing, the null hypothesis H_0 represents that the observation data \mathbf{x} is only the clutter \mathbf{c} and the alternative hypothesis H_1 represents that \mathbf{x} contains both the target signal \mathbf{s} and the clutter \mathbf{c} , namely

$$\begin{cases} H_0 : \begin{cases} \text{target is absent,} \\ \mathbf{x} = \mathbf{c}, \end{cases} \\ H_1 : \begin{cases} \text{target is present,} \\ \mathbf{x} = \xi \mathbf{s} + \mathbf{c}, \end{cases} \end{cases} \quad (2.1)$$

where ξ denotes the unknown amplitude coefficient which is complex scalar-valued. The observation data \mathbf{x} and the target signal \mathbf{s} denoting the steering vector are respectively given by

$$\begin{aligned} \mathbf{x} &= (x_0, \dots, x_{N-1})^T \in \mathbb{C}^N, \\ \mathbf{s} &= \frac{1}{\sqrt{N}} (1, \exp(-i 2\pi f_d), \dots, \exp(-i 2\pi f_d(N-1)))^T, \end{aligned}$$

where \mathbb{C}^N represents the N dimensional complex space, i denotes the imaginary unit, f_d is the signal normalized Doppler frequency, and $(\cdot)^T$ denotes the transpose of matrices or vectors. Conventional SCM estimator, derived by secondary data set $\{\mathbf{x}_i\}_{i=1}^m$, is given by [15]

$$\mathbf{R}_{\text{SCM}} = \frac{1}{m} \sum_{i=1}^m \mathbf{x}_i \mathbf{x}_i^H, \quad \mathbf{x}_i \in \mathbb{C}^N, \quad (2.2)$$

where $(\cdot)^H$ represents the conjugate transpose of matrices or vectors. This estimator has been widely utilized; for instance, the GLRT detector reads [21]

$$\frac{|\mathbf{x}_i^H \mathbf{R}_{\text{SCM}}^{-1} \mathbf{s}|^2}{\mathbf{s}^H \mathbf{R}_{\text{SCM}}^{-1} \mathbf{s}} \underset{H_0}{\overset{H_1}{\gtrless}} \gamma, \quad (2.3)$$

where γ denotes the detection threshold.

In the matrix-CFAR, to determine whether \mathbf{x} includes \mathbf{s} or not, we model the data by the covariance matrix as a Toeplitz HPD matrix. The covariance matrix of the observation data is defined as

$$\mathbf{R} = \begin{pmatrix} r_0 & \cdots & \bar{r}_k & \cdots & \bar{r}_{N-1} \\ \vdots & \ddots & \ddots & \ddots & \vdots \\ r_k & \ddots & r_0 & \ddots & \bar{r}_k \\ \vdots & \ddots & \ddots & \ddots & \vdots \\ r_{N-1} & \cdots & r_k & \cdots & r_0 \end{pmatrix} \in \mathcal{P}(N, \mathbb{C}), \quad (2.4)$$

where $\mathcal{P}(N, \mathbb{C})$ denotes the space of $N \times N$ HPD matrices, the component

$$r_k = \mathbb{E}[x_l \bar{x}_{l+k}], \quad 0 \leq k \leq N-1, \quad 0 \leq l \leq N-l-1 \quad (2.5)$$

is the k -th correlation coefficient. Here, \bar{r}_k is the conjugate of r_k , and $\mathbb{E}[\cdot]$ is the statistical expectation. Based on the ergodicity of a stationary process, each component r_l can be approximated by observation data as

$$r_k = \frac{1}{N} \sum_{l=0}^{N-1-k} x_l \bar{x}_{l+k}, \quad 0 \leq k \leq N-1. \quad (2.6)$$

The covariance matrix of clutter is estimated as \mathbf{R}_g by the observations $\{\mathbf{R}_i\}_{i=1}^m$. Consequently, the detection problem can be modeled as

$$\begin{cases} H_0 : \mathbf{R}_{\text{CUT}} = \mathbf{R}_g, \\ H_1 : \mathbf{R}_{\text{CUT}} \neq \mathbf{R}_g, \end{cases} \quad (2.7)$$

where the matrix \mathbf{R}_{CUT} is the covariance matrix of the observation in the cell under test (CUT). By defining a threshold γ , the signal detection is modeled as discriminating \mathbf{R}_{CUT} from \mathbf{R}_g by

$$d(\mathbf{R}_g, \mathbf{R}_{\text{CUT}}) \underset{H_0}{\overset{H_1}{\gtrless}} \gamma, \quad (2.8)$$

where $d(\mathbf{R}_g, \mathbf{R}_{\text{CUT}})$ is the difference between \mathbf{R}_{CUT} and \mathbf{R}_g , such as the Riemannian distance or TBD divergences that we are going to introduce in the next section.

The matrix-CFRA illustrated by Fig. 1 is summarized up as follows. Estimator of covariance matrices $\{\mathbf{R}_i\}_{i=1}^m$ of the observation data $\{\mathbf{x}_i\}_{i=1}^m$ is firstly calculated by (2.4) and (2.6). Mean or median \mathbf{R}_g of those covariance matrices will be obtained by using either the distance or divergences. The matrix \mathbf{R}_g can be considered as an estimator of the covariance matrix of the clutter since we consider almost all observation data $\{\mathbf{x}_i\}_{i=1}^m$ as the clutter, that is essential in design of the matrix-CFRA. The detection decision is performed by the comparison of the distance or difference of \mathbf{R}_{CUT} and \mathbf{R}_g and the threshold γ .

3 Means and medians of HPD matrices

In this section, we briefly introduce geometric means and medians in HPD spaces equipped with either the AIRM as Riemannian manifolds or the Frobenius metric as metric spaces. In the latter, divergence functions can be defined, playing the role of measuring the difference of two HPD matrices.

3.1 HPD manifolds and the RD mean and median

We firstly define the AIRM on the HPD matrix manifold $\mathcal{P}(N, \mathbb{C})$, and introduce the corresponding geodesic distance, also called the Riemannian distance. The tangent space at a point $\mathbf{P} \in \mathcal{P}(N, \mathbb{C})$

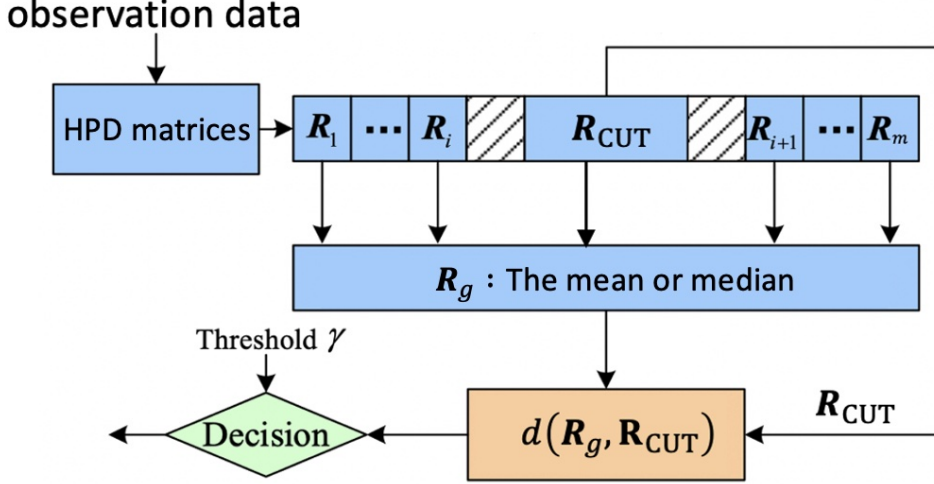


Figure 1: The process of matrix-CFAR.

is $T_{\mathbf{P}}\mathcal{P}(N, \mathbb{C}) \cong \mathcal{H}(N, \mathbb{C})$, which denotes the space of $N \times N$ Hermitian matrices. The tangent bundle is denoted by $T\mathcal{P}(N, \mathbb{C}) = \cup_{\mathbf{P}} T_{\mathbf{P}}\mathcal{P}(N, \mathbb{C})$. The well-known AIRM is defined by

$$\langle \mathbf{A}, \mathbf{B} \rangle_{\mathbf{P}} := \text{tr}(\mathbf{P}^{-1} \mathbf{A} \mathbf{P}^{-1} \mathbf{B}) \quad (3.1)$$

for $\mathbf{A}, \mathbf{B} \in T_{\mathbf{P}}\mathcal{P}(N, \mathbb{C})$, where tr denotes the trace of a matrix. The geodesic curve between two points $\mathbf{P}_0, \mathbf{P}_1 \in \mathcal{P}(N, \mathbb{C})$ is given by

$$\mathbf{P}(t) = \mathbf{P}_0^{\frac{1}{2}} \exp\left(t \mathbf{P}_0^{\frac{1}{2}} \text{Log}\left(\mathbf{P}_0^{-\frac{1}{2}} \mathbf{P}_1 \mathbf{P}_0^{-\frac{1}{2}}\right) \mathbf{P}_0^{\frac{1}{2}}\right) \mathbf{P}_0^{\frac{1}{2}}, \quad t \in [0, 1], \quad (3.2)$$

where \exp denotes matrix exponential and Log denotes the principal logarithm [16]. Obviously, $\mathbf{P}(0) = \mathbf{P}_0$, and $\mathbf{P}(1) = \mathbf{P}_1$. Under the AIRM metric, the geodesic distance between two points $\mathbf{P}_0, \mathbf{P}_1 \in \mathcal{P}(N, \mathbb{C})$ is given by

$$\begin{aligned} d_R(\mathbf{P}_0, \mathbf{P}_1) &= \left\| \text{Log}\left(\mathbf{P}_0^{-\frac{1}{2}} \mathbf{P}_1 \mathbf{P}_0^{-\frac{1}{2}}\right) \right\| \\ &= \left\| \text{Log}(\mathbf{P}_1^{-1} \mathbf{P}_0) \right\|, \end{aligned} \quad (3.3)$$

where $\|\cdot\|$ is the Frobenius norm associated to the Frobenius metric $\langle \mathbf{A}, \mathbf{B} \rangle := \text{tr}(\mathbf{A}^H \mathbf{B})$. For more details, the reader may refer to [27].

In the Riemannian manifold $\mathcal{P}(N, \mathbb{C})$ equipped with the AIRM, the exponential map $\text{Exp} : T\mathcal{P}(N, \mathbb{C}) \rightarrow \mathcal{P}(N, \mathbb{C})$ is defined by making use of the geodesics. Locally, assuming $\mathbf{P}(t)$ is the geodesic (3.2) connecting two arbitrary HPD matrices $\mathbf{P}_0 = \mathbf{P}(0)$, $\mathbf{P}_1 = \mathbf{P}(1)$, the exponential map gives endpoint of the geodesic, namely

$$\begin{aligned} \text{Exp}\left(\mathbf{P}_0, \dot{\mathbf{P}}(0)\right) &= \mathbf{P}_1 \\ &= \mathbf{P}_0^{\frac{1}{2}} \exp\left(\mathbf{P}_0^{\frac{1}{2}} \text{Log}\left(\mathbf{P}_0^{-\frac{1}{2}} \mathbf{P}_1 \mathbf{P}_0^{-\frac{1}{2}}\right) \mathbf{P}_0^{\frac{1}{2}}\right) \mathbf{P}_0^{\frac{1}{2}} \\ &= \mathbf{P}_0^{\frac{1}{2}} \exp\left(\mathbf{P}_0^{-\frac{1}{2}} \dot{\mathbf{P}}(0) \mathbf{P}_0^{-\frac{1}{2}}\right) \mathbf{P}_0^{\frac{1}{2}}. \end{aligned}$$

Using the Riemannian distance (3.3), we recall the RD mean and median of m HPD matrices $\{\mathbf{R}_i\}_{i=1}^m$ as follows

$$\bar{\mathbf{R}}_{\text{RDmean}} := \arg \min_{\mathbf{R} \in \mathcal{P}(N, \mathbb{C})} \frac{1}{m} \sum_{i=1}^m d_R^2(\mathbf{R}, \mathbf{R}_i), \quad (3.4)$$

$$\bar{\mathbf{R}}_{\text{RDmedian}} := \arg \min_{\mathbf{R} \in \mathcal{P}(N, \mathbb{C})} \frac{1}{m} \sum_{i=1}^m d_R(\mathbf{R}, \mathbf{R}_i). \quad (3.5)$$

In other words, the RD mean and median are, respectively, solutions of the optimization prob-

lems with objective functions

$$G_{\text{RDmean}}(\mathbf{R}) = \frac{1}{m} \sum_{i=1}^m d_R^2(\mathbf{R}, \mathbf{R}_i), \quad (3.6)$$

$$G_{\text{RDmedian}}(\mathbf{R}) = \frac{1}{m} \sum_{i=1}^m d_R(\mathbf{R}, \mathbf{R}_i). \quad (3.7)$$

Proposition 1. Since the RD mean and median are related to optimisation problems on HPD spaces as Riemannian manifolds, it is natural to propose the Riemannian gradient descent algorithms, i.e., gradient descent algorithms on Riemannian manifolds [8, 14]:

$$\begin{aligned} \mathbf{R}_{t+1} &= \text{Exp}(\mathbf{R}_t, -\eta_t \text{grad } G_{\text{RDmean}}(\mathbf{R}_t)) \\ &= \mathbf{R}_t^{\frac{1}{2}} \exp\left(-\eta_t \mathbf{R}_t^{-\frac{1}{2}} \text{grad } G_{\text{RDmean}}(\mathbf{R}_t) \mathbf{R}_t^{-\frac{1}{2}}\right) \mathbf{R}_t^{\frac{1}{2}} \\ &= \mathbf{R}_t^{\frac{1}{2}} \exp\left(-\eta_t \sum_{i=1}^m \text{Log}\left(\mathbf{R}_t^{-\frac{1}{2}} \mathbf{R}_i \mathbf{R}_t^{-\frac{1}{2}}\right)\right) \mathbf{R}_t^{\frac{1}{2}} \end{aligned}$$

and

$$\begin{aligned} \mathbf{R}_{t+1} &= \text{Exp}(\mathbf{R}_t, -\eta_t \text{grad } G_{\text{RDmedian}}(\mathbf{R}_t)) \\ &= \mathbf{R}_t^{\frac{1}{2}} \exp\left(-\eta_t \mathbf{R}_t^{-\frac{1}{2}} \text{grad } G_{\text{RDmedian}}(\mathbf{R}_t) \mathbf{R}_t^{-\frac{1}{2}}\right) \mathbf{R}_t^{\frac{1}{2}} \\ &= \mathbf{R}_t^{\frac{1}{2}} \exp\left(-\eta_t \sum_{i=1}^m \frac{\text{Log}\left(\mathbf{R}_t^{-\frac{1}{2}} \mathbf{R}_i \mathbf{R}_t^{-\frac{1}{2}}\right)}{d_R(\mathbf{R}_t, \mathbf{R}_i)}\right) \mathbf{R}_t^{\frac{1}{2}}. \end{aligned}$$

Here η_t is the step size, and grad denotes the Riemannian gradient on Riemannian manifolds.

For more details on Riemannian gradient descent algorithms, the reader may refer to [30, 31]. The RD mean and median can also be calculated numerically through the fixed-point algorithms [17]. It was noted that the detection performance of the RD mean in the matrix-CFAR is better than that of the RD median [17].

3.2 The total Bregman divergence, TBD means and medians

The Bregman divergence for matrices was introduced [13] and this idea has been extended to total Bregman divergences [20]. The total Bregman divergence of two matrices $\mathbf{A}, \mathbf{B} \in \text{GL}(N, \mathbb{C})$, the general linear group of $N \times N$ invertible complex-valued matrices, is defined by

$$\delta_F(\mathbf{A}, \mathbf{B}) = \frac{F(\mathbf{A}) - F(\mathbf{B}) - \langle \nabla F(\mathbf{B}), \mathbf{A} - \mathbf{B} \rangle}{\sqrt{1 + \|\nabla F(\mathbf{B})\|^2}}, \quad (3.8)$$

where $F(\mathbf{A})$ is a differentiable and strictly convex function in $\text{GL}(N, \mathbb{C})$ and ∇ denotes the (Euclidean) gradient with respect to the Frobenius metric, defined by

$$\langle \nabla F(\mathbf{A}), \mathbf{B} \rangle = \left. \frac{d}{d\varepsilon} \right|_{\varepsilon=0} F(\mathbf{A} + \varepsilon \mathbf{B}), \quad \mathbf{A}, \mathbf{B} \in \text{GL}(N, \mathbb{C}). \quad (3.9)$$

The well-known total square loss (TSL), and the total log-determinant (TLD) and total von-Neumann (TVN) divergences defined in the HPD manifold $\mathcal{P}(N, \mathbb{C})$ are shown in Table 1.

Before introducing the TBD medians, we briefly recall their mean counterparts. Details can be found in [20]. The TBD mean of m HPD matrices $\{\mathbf{R}_i\}_{i=1}^m$ is defined by

$$\arg \min_{\mathbf{R} \in \mathcal{P}(N, \mathbb{C})} \frac{1}{m} \sum_{i=1}^m \delta_F(\mathbf{R}, \mathbf{R}_i). \quad (3.10)$$

As the TBD $\delta_F(\mathbf{R}, \mathbf{R}_i)$ is defined in the convex HPD space and is strictly convex with respect to \mathbf{R} , the TBD mean exists uniquely. It solves the next matrix equation,

$$\nabla F(\mathbf{R}) = \left(\sum_{j=1}^m \frac{1}{\sqrt{1 + \|\nabla F(\mathbf{R}_j)\|^2}} \right)^{-1} \left(\sum_{i=1}^m \frac{\nabla F(\mathbf{R}_i)}{\sqrt{1 + \|\nabla F(\mathbf{R}_i)\|^2}} \right). \quad (3.11)$$

Table 1: The TBDs

	The function $F(\mathbf{Y})$	TBDs in $\mathcal{P}(N, \mathbb{C})$
TSL	$\frac{1}{2} \ \mathbf{Y}\ ^2$	$\delta_{\text{TSL}}(\mathbf{Y}, \mathbf{Z}) = \frac{\ \mathbf{Y} - \mathbf{Z}\ ^2}{2\sqrt{1 + \ \mathbf{Z}\ ^2}}$
TLD divergence	$-\ln \det \mathbf{Y}$	$\delta_{\text{TLD}}(\mathbf{Y}, \mathbf{Z}) = \frac{\ln \det(\mathbf{Z}\mathbf{Y}^{-1}) + \text{tr}(\mathbf{Z}^{-1}\mathbf{Y}) - N}{2\sqrt{1 + \ \mathbf{Z}^{\text{H}}\ ^2}}$
TVN divergence	$\text{tr}(\mathbf{Y} \text{Log } \mathbf{Y} - \mathbf{Y})$	$\delta_{\text{TVN}}(\mathbf{Y}, \mathbf{Z}) = \frac{\text{tr}(\mathbf{Y}(\text{Log } \mathbf{Y} - \text{Log } \mathbf{Z}) - \mathbf{Y} + \mathbf{Z})}{2\sqrt{1 + \ (\text{Log } \mathbf{Z})^{\text{H}}\ ^2}}$

In particular, the TBD means corresponding to the convex functions F given by Table 1 can be calculated analytically [20]. We summarize them up as follows. The TSL mean, TLD mean, and TVN mean of m HPD matrices $\{\mathbf{R}_i\}_{i=1}^m$ are respectively given by

$$\bar{\mathbf{R}}_{\text{TSL}} = \left(\sum_{j=1}^m \frac{1}{\sqrt{1 + \|\mathbf{R}_j\|^2}} \right)^{-1} \left(\sum_{i=1}^m \frac{\mathbf{R}_i}{\sqrt{1 + \|\mathbf{R}_i\|^2}} \right), \quad (3.12)$$

$$\bar{\mathbf{R}}_{\text{TLD}} = \left(\sum_{j=1}^m \frac{1}{\sqrt{1 + \|\mathbf{R}_j^{-1}\|^2}} \right)^{-1} \left(\sum_{i=1}^m \frac{\mathbf{R}_i^{-1}}{\sqrt{1 + \|\mathbf{R}_i^{-1}\|^2}} \right)^{-1}, \quad (3.13)$$

$$\bar{\mathbf{R}}_{\text{TVN}} = \exp \left(\left(\sum_{j=1}^m \frac{1}{\sqrt{1 + \|\text{Log } \mathbf{R}_j\|^2}} \right)^{-1} \sum_{i=1}^m \frac{\text{Log } \mathbf{R}_i}{\sqrt{1 + \|\text{Log } \mathbf{R}_i\|^2}} \right). \quad (3.14)$$

Definition 2. Assume F is a differentiable and strictly convex function. Let δ_F be the associated TBD. The TBD median of m HPD matrices $\{\mathbf{R}_i\}_{i=1}^m$ is defined by

$$\arg \min_{\mathbf{R} \in \mathcal{P}(N, \mathbb{C})} \frac{1}{m} \sum_{i=1}^m \{\delta_F(\mathbf{R}, \mathbf{R}_i)\}^{\frac{1}{2}}. \quad (3.15)$$

Theorem 3. If the TBD median (3.15) exists, then it satisfies the matrix equation,

$$\nabla F(\mathbf{R}) = \left(\sum_{j=1}^m \frac{1}{\{\delta_F(\mathbf{R}, \mathbf{R}_j)\}^{\frac{1}{2}} \sqrt{1 + \|\nabla F(\mathbf{R}_j)\|^2}} \right)^{-1} \left(\sum_{i=1}^m \frac{\nabla F(\mathbf{R}_i)}{\{\delta_F(\mathbf{R}, \mathbf{R}_i)\}^{\frac{1}{2}} \sqrt{1 + \|\nabla F(\mathbf{R}_i)\|^2}} \right). \quad (3.16)$$

Proof. Let $G(\mathbf{R})$ be the function to be optimized, namely

$$G(\mathbf{R}) := \frac{1}{m} \sum_{i=1}^m \{\delta_F(\mathbf{R}, \mathbf{R}_i)\}^{\frac{1}{2}}. \quad (3.17)$$

The proof is completed by setting $\nabla G(\mathbf{R}) = 0$ where the gradient of $G(\mathbf{R})$ is

$$\nabla G(\mathbf{R}) = \frac{1}{2m} \sum_{i=1}^m \frac{\nabla F(\mathbf{R}) - \nabla F(\mathbf{R}_i)}{\{\delta_F(\mathbf{R}, \mathbf{R}_i)\}^{\frac{1}{2}} \sqrt{1 + \|\nabla F(\mathbf{R}_i)\|^2}}. \quad (3.18)$$

□

Unfortunately, it is difficult to solve the matrix equation (3.16) analytically, and alternatively we seek for its numerical solutions using the fixed-point algorithm [26].

Proposition 4. The TSL median, the TLD median, and the TVN median of m HPD matrices $\{\mathbf{R}_i\}_{i=1}^m$ can respectively be calculated by the following fixed-point algorithms in Table 2.

In the matrix-CFAR, the matrix \mathbf{R}_g in (2.8) will be replaced by the TBD means, the TBD medians, the RD mean, and so forth; see also Fig. 1. Numerical simulations in the following sections show that the fixed-point algorithms are convergent.

Table 2: The fixed-point algorithms for computing TBD medians

TBD	The fixed-point algorithm
TSL	$\bar{\mathbf{R}}_{t+1} = \left(\sum_{j=1}^m \frac{1}{\{\delta_{\text{TSL}}(\bar{\mathbf{R}}_t, \mathbf{R}_j)\}^{\frac{1}{2}} \sqrt{1 + \ \mathbf{R}_j\ ^2}} \right)^{-1} \left(\sum_{i=1}^m \frac{\mathbf{R}_i}{\{\delta_{\text{TSL}}(\bar{\mathbf{R}}_t, \mathbf{R}_i)\}^{\frac{1}{2}} \sqrt{1 + \ \mathbf{R}_i\ ^2}} \right)$
TLD	$\bar{\mathbf{R}}_{t+1} = \left(\sum_{j=1}^m \frac{1}{\{\delta_{\text{TLD}}(\bar{\mathbf{R}}_t, \mathbf{R}_j)\}^{\frac{1}{2}} \sqrt{1 + \ \mathbf{R}_j^{-1}\ ^2}} \right) \left(\sum_{i=1}^m \frac{\mathbf{R}_i^{-1}}{\{\delta_{\text{TLD}}(\bar{\mathbf{R}}_t, \mathbf{R}_i)\}^{\frac{1}{2}} \sqrt{1 + \ \mathbf{R}_i^{-1}\ ^2}} \right)^{-1}$
TVN	$\bar{\mathbf{R}}_{t+1} = \exp \left(\left(\sum_{j=1}^m \frac{1}{\{\delta_{\text{TVN}}(\bar{\mathbf{R}}_t, \mathbf{R}_j)\}^{\frac{1}{2}} \sqrt{1 + \ (\text{Log } \mathbf{R}_j)^{\text{H}}\ ^2}} \right)^{-1} \sum_{i=1}^m \frac{\text{Log } \mathbf{R}_i}{\{\delta_{\text{TVN}}(\bar{\mathbf{R}}_t, \mathbf{R}_i)\}^{\frac{1}{2}} \sqrt{1 + \ (\text{Log } \mathbf{R}_i)^{\text{H}}\ ^2}} \right)$

4 Numerical performance analysis

To confirm and compare the performance of the matrix-CFAR via TBD means and medians, the following numerical simulations are conducted. For the comparison, we also show results of the RD mean induced from the AIRM, and the GLRT. We consider clutter as the compound-Gaussian clutter which is a model commonly used for characterizing heavy-tailed clutter distributions, in particular sea clutter [33], defined by

$$\mathbf{c} = \sqrt{\tau} \mathbf{z}. \quad (4.1)$$

Here \mathbf{z} is called the speckle component which is fast fluctuating and modeled by an N dimensional random complex vector possessing the complex circular Gaussian distribution $CN(0, \mathbf{\Sigma})$ of zero-mean and a covariance matrix $\mathbf{\Sigma}$. Its probability density function is given by

$$p(\mathbf{z} | 0, \mathbf{\Sigma}) = \frac{1}{\pi^N \det(\mathbf{\Sigma})} \exp(-\mathbf{z}^{\text{H}} \mathbf{\Sigma}^{-1} \mathbf{z}). \quad (4.2)$$

The positive real random variable τ is called the texture component which is comparatively slowly varying. In the simulation, the texture component τ is assumed to subject to a gamma distribution with a shape parameter α and a scale parameter β whose probability density function is

$$q(\tau | \alpha, \beta) = \frac{1}{\beta^\alpha \Gamma(\alpha)} \tau^{\alpha-1} \exp\left(-\frac{\tau}{\beta}\right), \quad (4.3)$$

where $\Gamma(\cdot)$ denotes the gamma function. Consequently, the distribution of clutter is defined by the complex K-distribution which is a special compound-Gaussian model [33]. In the simulation, we generate the speckle component from $CN(0, \mathbf{\Sigma})$ of which the known covariance matrix $\mathbf{\Sigma}$ is given by

$$\mathbf{\Sigma} = \mathbf{\Sigma}_0 + \mathbf{I}_N \quad (4.4)$$

where

$$\mathbf{\Sigma}_0(i, j) = \sigma_c^2 \rho^{|i-j|} \exp(i2\pi f_c(i-j)), \quad i, j = 1, 2, \dots, N.$$

Here, \mathbf{I}_N is the N dimensional identity matrix. In the simulation, the clutter-to-noise ratio σ_c is set to $\sigma_c^2 = 20\text{dB}$, the one-lag coefficient is $\rho = 0.9$, and the normalized Doppler frequency of clutter is $f_c = 0.2$. Furthermore, the shape parameter is set to $\alpha = 4$ and the scale parameter is set to $\beta = 3$.

Furthermore, the false alarm rate P_{fa} is 10^{-3} , and the signal normalized Doppler frequency f_d is 0.2. The dimension of the signal, N , and the number of the observation, m , are both 8. The threshold γ is derived by $100/P_{fa}$, and the probability of detection P_d is derived by 2000 independent trails. Fig. 2 shows that the TBD means and medians are advantageous over the RD mean, median and the GLRT. In particular, the TVN median has the best performance, the TLD median behaves better than the TLD mean, but surprisingly the TSL median is worse than the TSL mean.

5 Robust analysis

In real detection, the received signal may also include outliers, and hence robustness about estimate of the covariance matrix is crucial. To evaluate the robustness of the detectors to outliers, the

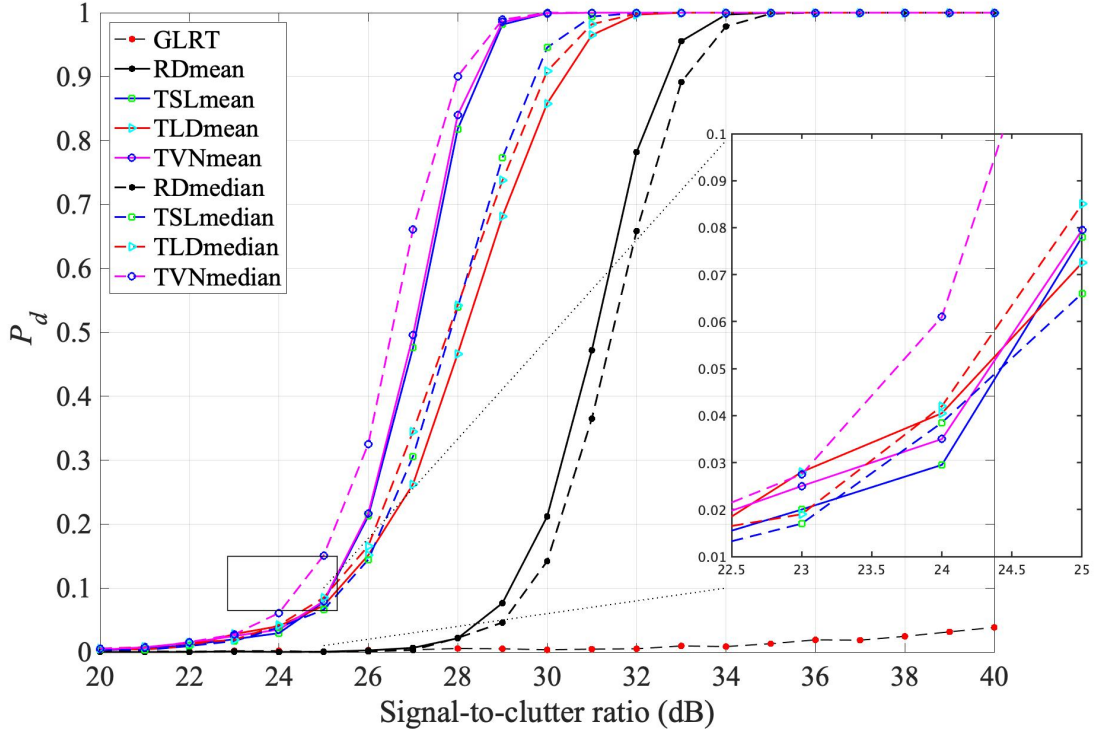


Figure 2: P_d versus signal-to-clutter ratio for the TBD means and medians, the RD mean and median and the GLRT detector.

influence function has usually been employed [20]. It was noted that the influence functions with respect to the TSL mean and the TLD mean can easily be calculated analytically but not for the TVN mean [20]. The situation for the median counterparts is often more complicated. In this section, we will propose an orthogonal basis for Hermitian matrices; by doing so, we are allowed to rewrite the equations of influence functions as a linear system, that can be solved analytically in a routine manner.

5.1 An orthogonal basis for Hermitian matrices

As we will see later that influences functions are defined as a small perturbation of the means or medians that depends on a Hermitian matrix. A well-known basis for the N^2 dimensional space of Hermitian matrices $\mathcal{H}(N, \mathbb{C})$ is given by N^2 number of matrices:

$$\begin{aligned} \mathbf{E}_{ii}, & \quad 1 \leq i \leq N; \\ \mathbf{E}_{ij} + \mathbf{E}_{ji}, & \quad 1 \leq i < j \leq N; \\ i(\mathbf{E}_{ij} - \mathbf{E}_{ji}), & \quad 1 \leq i < j \leq N, \end{aligned} \quad (5.1)$$

where \mathbf{E}_{ij} represents the $N \times N$ matrix with 1 at row i and column j and 0 elsewhere. To ease the application in the following robust analysis, we normalize them into the following orthogonal basis

$$\begin{aligned} \mathbf{E}_{ii}, & \quad 1 \leq i \leq N; \\ \frac{1}{\sqrt{2}}(\mathbf{E}_{ij} + \mathbf{E}_{ji}), & \quad 1 \leq i < j \leq N; \\ \frac{i}{\sqrt{2}}(\mathbf{E}_{ij} - \mathbf{E}_{ji}), & \quad 1 \leq i < j \leq N, \end{aligned} \quad (5.2)$$

and denote it by $\{\mathbf{E}_k\}_{k=1}^{N^2}$. Each Hermitian matrix $\mathbf{H} \in \mathcal{H}(N, \mathbb{C})$ can be represented as a linear combination using the orthogonal basis, namely

$$\mathbf{H} = h^k \mathbf{E}_k, \quad h^k \in \mathbb{R}, \quad (5.3)$$

where the summation is over $\{1, \dots, N^2\}$ and the Einstein summation convention is applied here and all through the paper. It is immediate to check that the basis $\{\mathbf{E}_k\}_{k=1}^{N^2}$ is orthogonal by showing

that

$$\langle \mathbf{E}_k, \mathbf{E}_l \rangle = \delta_{kl}, \quad \forall k, l = 1, \dots, N^2, \quad (5.4)$$

where δ_{kl} is the Kronecker delta that gives 1 when $k = l$ and 0 otherwise. Given a Hermitian matrix \mathbf{H} , it is immediate to write down its coordinate expression as

$$\mathbf{H} = h^k \mathbf{E}_k, \quad \text{with } h^k = \langle \mathbf{H}, \mathbf{E}_k \rangle. \quad (5.5)$$

5.2 Robustness via influence functions

Let $\bar{\mathbf{R}}$ be the TBD medians (or TBD means, RD mean, RD median) of a given set of m HPD matrices $\{\mathbf{R}_i\}_{i=1}^m$, and let $\hat{\mathbf{R}}$ be the TBD medians (or TBD means, RD mean, RD median) of the mixed HPD data including n number of outliers $\{\mathbf{P}_j\}_{j=1}^n$. By thinking of the outliers as a perturbation ε ($\varepsilon \ll 1$) of each mean or median, $\hat{\mathbf{R}}$ and $\bar{\mathbf{R}}$ can be related by

$$\hat{\mathbf{R}} = \bar{\mathbf{R}} + \varepsilon \mathbf{H} (\{\mathbf{R}_i\}_{i=1}^m, \{\mathbf{P}_j\}_{j=1}^n) + \mathcal{O}(\varepsilon^2), \quad (5.6)$$

where $\mathbf{H} (\{\mathbf{R}_i\}_{i=1}^m, \{\mathbf{P}_j\}_{j=1}^n)$ is a Hermitian matrix depending on the outliers, and the m HPD matrices $\{\mathbf{R}_i\}_{i=1}^m$, the latter of which are assumed to be given and fixed. The function

$$f (\{\mathbf{R}_i\}_{i=1}^m, \{\mathbf{P}_j\}_{j=1}^n) := \frac{\|\mathbf{H} (\{\mathbf{R}_i\}_{i=1}^m, \{\mathbf{P}_j\}_{j=1}^n)\|}{\|\bar{\mathbf{R}}\|} \quad (5.7)$$

is defined as the (normalized) *influence function*.

To calculate the corresponding influence functions, define the objective function $G(\mathbf{R})$ for the contaminated $m + n$ number of HPD matrices as follows

$$G(\mathbf{R}) := (1 - \varepsilon) \frac{1}{m} \sum_{i=1}^m d(\mathbf{R}, \mathbf{R}_i) + \varepsilon \frac{1}{n} \sum_{j=1}^n d(\mathbf{R}, \mathbf{P}_j), \quad (5.8)$$

where d is either the distance or divergence functions for medians, and square of them for means. Since $\hat{\mathbf{R}}$ is any mean or median of the mixed $m + n$ HPD matrices, we have $\nabla G(\hat{\mathbf{R}}) = \mathbf{0}$,¹ that is,

$$(1 - \varepsilon) \frac{1}{m} \sum_{i=1}^m \nabla d(\hat{\mathbf{R}}, \mathbf{R}_i) + \varepsilon \frac{1}{n} \sum_{j=1}^n \nabla d(\hat{\mathbf{R}}, \mathbf{P}_j) = \mathbf{0}. \quad (5.9)$$

Differentiating $\nabla G(\hat{\mathbf{R}}) = \mathbf{0}$ about ε at $\varepsilon = 0$, we obtain a matrix equation for \mathbf{H} :

$$\frac{1}{m} \frac{d}{d\varepsilon} \Big|_{\varepsilon=0} \left(\sum_{i=1}^m \nabla d(\hat{\mathbf{R}}, \mathbf{R}_i) \right) + \frac{1}{n} \sum_{j=1}^n \nabla d(\bar{\mathbf{R}}, \mathbf{P}_j) = \mathbf{0}. \quad (5.10)$$

Next, we are going to show that the above equation can be solved analytically using the orthogonal basis (5.2) defined above.

Recall that the gradient of a function defined in HPD spaces is a Hermitian matrix. Using the orthogonal basis $\{\mathbf{E}_k\}_{k=1}^{N^2}$, we can write

$$\sum_{i=1}^m \nabla d(\hat{\mathbf{R}}, \mathbf{R}_i) = \xi^l(\hat{\mathbf{R}}) \mathbf{E}_l \quad (5.11)$$

and

$$\sum_{j=1}^n \nabla d(\bar{\mathbf{R}}, \mathbf{P}_j) = \phi^l \mathbf{E}_l. \quad (5.12)$$

Letting $\mathbf{H} = h^s \mathbf{E}_s$, the first term in (5.10) then becomes

$$\begin{aligned} \frac{1}{m} \frac{d}{d\varepsilon} \Big|_{\varepsilon=0} \xi^l(\hat{\mathbf{R}}) \mathbf{E}_l &= \frac{1}{m} \frac{d}{d\varepsilon} \Big|_{\varepsilon=0} \xi^l(\bar{\mathbf{R}} + \varepsilon \mathbf{H}) \mathbf{E}_l \\ &= \frac{1}{m} \langle \nabla \xi^l(\bar{\mathbf{R}}), \mathbf{H} \rangle \mathbf{E}_l \\ &= \frac{h^k}{m} \langle \nabla \xi^l(\bar{\mathbf{R}}), \mathbf{E}_k \rangle \mathbf{E}_l. \end{aligned} \quad (5.13)$$

¹Note that in the Riemannian case, this should be $\text{grad } G(\hat{\mathbf{R}}) = 0$, which is nevertheless equivalent to $\nabla G(\hat{\mathbf{R}}) = 0$ for HPD manifolds equipped with the AIRM.

Definition of the gradient (3.9) (induced to HPD spaces) is applied here. Although a linear system about $\{h^k\}_{k=1}^{N^2}$ can be obtained, unfortunately, as $\{\zeta^l(\bar{\mathbf{R}})\}_{l=1}^{N^2}$ is the coordinates whose gradient can be practically difficult to be calculated, in particular, in numerical simulations. Alternatively, noticing the first term in (5.10) is Hermitian and linear about $\{h^k\}_{k=1}^{N^2}$ (from (5.13)), we can simply write

$$\frac{d}{d\varepsilon}\bigg|_{\varepsilon=0} \left(\sum_{i=1}^m \nabla d(\hat{\mathbf{R}}, \mathbf{R}_i) \right) = h^k \theta_k^l \mathbf{E}_l. \quad (5.14)$$

Consequently, we have successfully written the matrix equation (5.10) as a linear system about $\{h^k\}_{k=1}^{N^2}$ with matrix coefficients:

$$\frac{1}{m} h^k \theta_k^l \mathbf{E}_l + \frac{1}{n} \phi^l \mathbf{E}_l = \mathbf{0}. \quad (5.15)$$

Conducting Frobenius metric on both sides with each \mathbf{E}_s and making use of the orthogonality, we obtain a linear system for $\{h^k\}_{k=1}^{N^2}$, reading

$$\frac{1}{m} \theta_k^s h^k + \frac{1}{n} \phi^s = 0, \quad s = 1, \dots, N^2, \quad (5.16)$$

which can be immediately solved if the coefficient matrix (θ_k^s) is invertible. We summarize the above deduction into the following theorem.

Theorem 5. Under the orthogonal basis $\{\mathbf{E}_k\}_{k=1}^{N^2}$ defined by (5.2), the Hermitian matrix $\mathbf{H} = h^k \mathbf{E}_k$ in the influence function (5.7) is given by linear system (5.16).

Influence function of the RD mean. Taking the RD mean as an illustrative example, we show how the above deduction helps us to derive the matrix \mathbf{H} and hence the corresponding influence function. Regarding the contaminated HPD matrices, define $G(\mathbf{R})$ as the objective function, i.e.,

$$G(\mathbf{R}) := (1 - \varepsilon) \frac{1}{m} \sum_{i=1}^m d_R^2(\mathbf{R}, \mathbf{R}_i) + \varepsilon \frac{1}{n} \sum_{j=1}^n d_R^2(\mathbf{R}, \mathbf{P}_j), \quad (5.17)$$

where

$$d_R^2(\mathbf{R}, \mathbf{R}_i) = \|\text{Log}(\mathbf{R}_i^{-1} \mathbf{R})\|^2 = \text{tr}(\text{Log}^2(\mathbf{R}_i^{-1} \mathbf{R})). \quad (5.18)$$

Differentiate grad $G(\hat{\mathbf{R}}) = \mathbf{0}$ with respect to ε at $\varepsilon = 0$ and obtain

$$\frac{1}{m} \frac{d}{d\varepsilon}\bigg|_{\varepsilon=0} \sum_{i=1}^m \hat{\mathbf{R}} \text{Log}(\mathbf{R}_i^{-1} \hat{\mathbf{R}}) + \frac{1}{n} \sum_{j=1}^n \bar{\mathbf{R}} \text{Log}(\mathbf{P}_j^{-1} \bar{\mathbf{R}}) = \mathbf{0}. \quad (5.19)$$

The second term can be simply written as

$$\frac{1}{n} \sum_{j=1}^n \bar{\mathbf{R}} \text{Log}(\mathbf{P}_j^{-1} \bar{\mathbf{R}}) = \frac{1}{n} \phi^k \mathbf{E}_k, \quad (5.20)$$

while the first term can be expanded as [20, 25]

$$\frac{1}{m} \sum_{i=1}^m \left(\mathbf{H} \text{Log}(\mathbf{R}_i^{-1} \bar{\mathbf{R}}) + \bar{\mathbf{R}} \int_0^1 [(\mathbf{R}_i^{-1} \bar{\mathbf{R}} - \mathbf{I})\tau + \mathbf{I}]^{-1} \mathbf{R}_i^{-1} \mathbf{H} [(\mathbf{R}_i^{-1} \bar{\mathbf{R}} - \mathbf{I})\tau + \mathbf{I}]^{-1} d\tau \right).$$

Substituting $\mathbf{H} = h^k \mathbf{E}_k$ to the first term, it can be written in the form $\frac{1}{m} h^k \theta_k^s \mathbf{E}_s$, where θ_k^s is given by

$$\theta_k^s = \left\langle \sum_{i=1}^m \left(\mathbf{E}_k \text{Log}(\mathbf{R}_i^{-1} \bar{\mathbf{R}}) + \bar{\mathbf{R}} \int_0^1 [(\mathbf{R}_i^{-1} \bar{\mathbf{R}} - \mathbf{I})\tau + \mathbf{I}]^{-1} \mathbf{R}_i^{-1} \mathbf{E}_k [(\mathbf{R}_i^{-1} \bar{\mathbf{R}} - \mathbf{I})\tau + \mathbf{I}]^{-1} d\tau \right), \mathbf{E}_s \right\rangle.$$

Finally, we obtain the linear system (5.16) about $\{h^k\}_{k=1}^{N^2}$ by conducting the Frobenius metric with respect to each element of the orthogonal basis, which will give us the influence function for the RD mean. Those of the RD median, as well as the TBD means and medians can also be analytically computed in a similar way; details are omitted here.

In the following simulations, we firstly generate m data of sample, each of which is N dimensional and complex valued, generated from $CN(0, \Sigma)$ where the covariance matrix Σ is given by

(4.4). The means and medians $\overline{\mathbf{R}}$ are calculated from the m HPD covariance matrices $\{\mathbf{R}_i\}_{i=1}^m$ of the m number of sample data. We then mix n outliers $\{\mathbf{P}_j\}_{j=1}^n$ with the sample data; the outliers are modeled as the covariance matrix of $\xi\mathbf{s} + \mathbf{c}$ where \mathbf{s} denotes the steering vector, \mathbf{c} is the Gaussian clutter with the covariance matrix $\mathbf{\Sigma}$, and ξ is the amplitude coefficient derived by the signal-to-clutter ratio which is set to 40 dB. In the numerical simulations, the number of sample is $m = 50$ while the number of outliers n are varying from 1 to 40. Fig. 3 plots the influence functions which are calculated by averaging 1000 trails and are shown in the logarithmic scale. We notice that the influence functions of the TBD medians are smaller than the TBD means. However, regardless of its worse detection performance compared with the TBD means and medians, the RD mean and median are more robust, although the RD mean and median take much longer time than the TBD means and medians. Therefore, from a comprehensive perspective the TBD medians can serve as effective estimators.

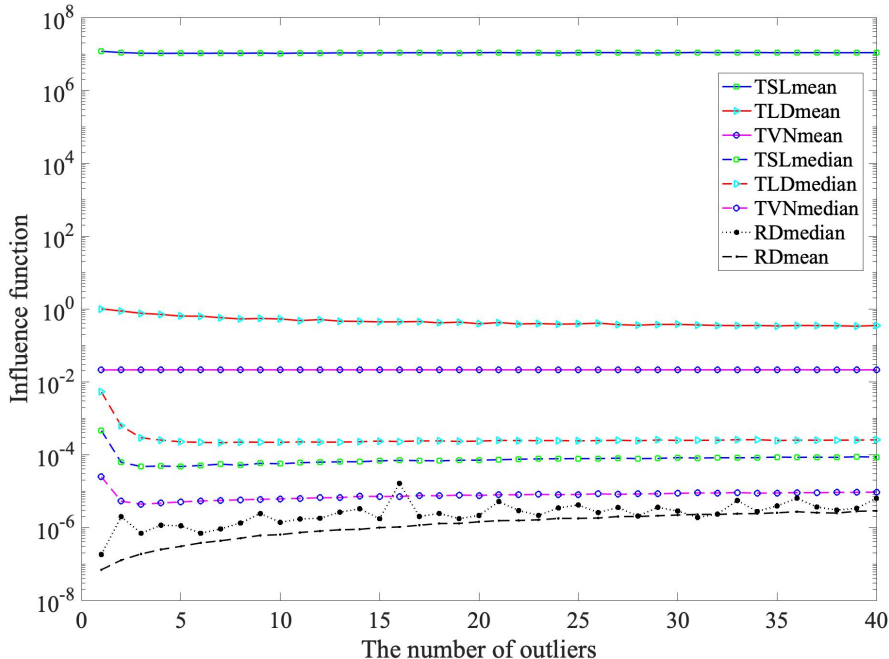


Figure 3: Robust analysis of the RD mean and median, and the TBD means and medians via the accurate influence functions.

6 Conclusion

The TBD medians were defined and applied to matrix-CFAR detectors corresponding to the well-known TBDs, i.e., the TSL, and the TLD and TVN divergences. To illustrate the improvement of detection performance, they were compared with their mean counterparts, the RD mean and median associated to the AIRM, as well as the conventional GLRT detector. Simulations showed that the TVN median performed the best from the viewpoint of probability of detection.

To analyze the robustness of those detectors to outliers, we transformed the intractable governing matrix equation into a linear system by introducing an orthogonal basis for Hermitian matrices. This allowed us to calculate the corresponding influence functions analytically and made the robust analysis accurate and precise. We believe this methodology works equally well for other geometric detectors in matrix-CFAR. By simulations, the RD mean is most robust among all of them, while the TBD medians are more robust compared with the TBD means. From an overall point of view, the TBD medians, in particular the TVN median, have best performance and satisfactory robustness.

As the optimization problem is convex and defined in a convex space, the TBD means exist uniquely. Unfortunately, an analytical verification of the existence and uniqueness of TBD medians is yet to be constructed, although numerical simulations suggest so. Future research in applications includes detection problems for real-world data using the TBD medians. Finally, it would also

be interesting to extend the current study to other covariance estimators, such as the diagonal loading [1, 11], and structured covariance interference (e.g., [9]).

Acknowledgements.

The authors thank Prof. Sergey Yurish for the kind invitation and for the hospitality during the ASPAI'2021 Conference, in which part of the work was presented. The authors would also like to thank Xiaoqiang Hua and Hiroki Sato for helpful discussions. This work was partially supported by Japan Society for the Promotion of Science KAKENHI (No. JP20K14365), Japan Science and Technology Agency CREST (No. JPMJCR1914), and the Fukuzawa Fund of Keio University.

References

- [1] Y. I. Abramovich, N. K. Spencer, and A. Y. Gorokhov. Modified GLRT and AMF framework for adaptive detectors. *IEEE Transactions on Aerospace and Electronic Systems*, 43(3):1017–1051, 2007.
- [2] F. Bandiera, O. Besson, and G. Ricci. Knowledge-aided covariance matrix estimation and adaptive detection in compound-Gaussian noise. *IEEE Transactions on Signal Processing*, 58(10):5391–5396, 2010.
- [3] F. Barbaresco. Innovative tools for radar signal processing based on Cartan's geometry of SPD matrices & information geometry. In *2008 IEEE International Radar Conference*, pages 1–6, 2008.
- [4] F. Barbaresco. Interactions between symmetric cone and information geometries: Bruhat-tits and siegel spaces models for high resolution autoregressive doppler imagery. In F. Nielsen, editor, *Emerging Trends In Visual Computing*, pages 124–163, Palaiseau, France, 2009.
- [5] F. Barbaresco and U. Meier. Radar monitoring of a wake vortex: Electromagnetic reflection of wake turbulence in clear air. *Comptes Rendus Physique*, 11(1):54–67, 2010.
- [6] O. Besson, J. Tourneret, and S. Bidon. Knowledge-aided Bayesian detection in heterogeneous environments. *IEEE Signal Processing Letters*, 14(5):355–358, 2007.
- [7] H. Chahrour, R. M. Dansereau, S. Rajan, and B. Balaji. Target detection through Riemannian geometric approach with application to drone detection. *IEEE Access*, 9:123950–123963, 2021.
- [8] M. Charfi, Z. Chebbi, M. Moakher, and B. C. Vemuri. Bhattacharyya median of symmetric positive-definite matrices and application to the denoising of diffusion-tensor fields. In *2013 IEEE 10th International Symposium on Biomedical Imaging*, pages 1227–1230, 2013.
- [9] D. Ciuonzo, D. Orlando, and L. Pallotta. On the maximal invariant statistic for adaptive radar detection in partially homogeneous disturbance with persymmetric covariance. *IEEE Signal Processing Letters*, 23(12):1830–1834, 2016.
- [10] A. De Maio, A. Farina, and G. Foglia. Knowledge-aided Bayesian radar detectors & their application to live data. *IEEE Transactions on Aerospace and Electronic Systems*, 46(1):170–183, 2010.
- [11] A. De Maio, L. Pallotta, J. Li, and P. Stoica. Loading factor estimation under affine constraints on the covariance eigenvalues with application to radar target detection. *IEEE Transactions on Aerospace and Electronic Systems*, 55(3):1269–1283, 2019.
- [12] A. Decurninge and F. Barbaresco. Robust Burg estimation of radar scatter matrix for autoregressive structured SIRV based on fréchet medians. *IET Radar, Sonar & Navigation*, 11(1):78–89, 2017.
- [13] I. S. Dhillon and J. A. Tropp. Matrix nearness problems with Bregman divergences. *SIAM Journal on Matrix Analysis and Applications*, 29(4):1120–1146, 2008.
- [14] P. T. Fletcher, S. Venkatasubramanian, and S. Joshi. Robust statistics on Riemannian manifolds via the geometric median. In *2008 IEEE Conference on Computer Vision and Pattern Recognition*, pages 1–8, 2008.
- [15] N. R. Goodman. Statistical analysis based on a certain multivariate complex Gaussian distribution. *The Annals of Mathematical Statistics*, 34(1):152–177, 1963.
- [16] N. J. Higham. *Functions of Matrices: Theory and Computation*. SIAM, Philadelphia, 2008.

- [17] X. Hua, Y. Cheng, H. Wang, Y. Qin, and Y. Li. Geometric means and medians with applications to target detection. *IET Signal Processing*, 11(6):711–720, 2017.
- [18] X. Hua, Y. Cheng, H. Wang, Y. Qin, Y. Li, and W. Zhang. Matrix CFAR detectors based on symmetrized Kullback–Leibler and total Kullback–Leibler divergences. *Digital Signal Processing*, 69:106–116, 2017.
- [19] X. Hua, H. Fan, Y. Cheng, H. Wang, and Y. Qin. Information geometry for radar target detection with total Jensen–Bregman divergence. *Entropy*, 20(4):256, 2018.
- [20] X. Hua, Y. Ono, L. Peng, Y. Cheng, and H. Wang. Target detection within nonhomogeneous clutter via total Bregman divergence-based matrix information geometry detectors. *IEEE Transactions on Signal Processing*, 69:4326–4340, 2021.
- [21] E. J. Kelly. Adaptive detection in non-stationary interference, part I and part II. Technical report, Lincoln Laboratory, MIT, June 25, 1985.
- [22] J. Lapuyade-Lahorgue and F. Barbaresco. Radar detection using Siegel distance between autoregressive processes, application to HF and X-band radar. In *2008 IEEE Radar Conference*, pages 1–6, 2008.
- [23] N. Li, H. Yang, G. Cui, L. Kong, and Q. H. Liu. Adaptive two-step Bayesian MIMO detectors in compound-Gaussian clutter. *Signal Processing*, 161:1–13, 2019.
- [24] M. Martorella, S. Gelli, and A. Bacci. Ground moving target imaging via SDAP-ISAR processing: Review and new trends. *Sensors*, 21(7):2391, 2021.
- [25] M. Moakher. A differential geometric approach to the geometric mean of symmetric positive-definite matrices. *SIAM Journal on Matrix Analysis and Applications*, 26(3):735–747, 2005.
- [26] M. Moakher. On the averaging of symmetric positive-definite tensors. *Journal of Elasticity*, 82(3):273–296, 2006.
- [27] M. Moakher and M. Zérai. The Riemannian geometry of the space of positive-definite matrices and its application to the regularization of positive-definite matrix-valued data. *Journal of Mathematical Imaging and Vision*, 40(2):171–187, 2011.
- [28] I. S. Reed, J. D. Mallett, and L. E. Brennan. Rapid convergence rate in adaptive arrays. *IEEE Transactions on Aerospace and Electronic Systems*, AES-10(6):853–863, 1974.
- [29] M. Richards. *Fundamentals of Radar Signal Processing*. McGraw-Hill Professional Professional, 2nd edition, 2014.
- [30] S. T. Smith. *Geometric Optimization Methods for Adaptive Filtering*. PhD Thesis, Harvard University, Cambridge, Massachusetts, 1993.
- [31] C. Udriște. *Convex Functions and Optimization Methods on Riemannian Manifolds*. Springer Science+Business Media, B.V., Dordrecht, 1994.
- [32] P. Wang, Z. Wang, H. Li, and B. Himed. Knowledge-aided parametric adaptive matched filter with automatic combining for covariance estimation. *IEEE Transactions on Signal Processing*, 62(18):4713–4722, 2014.
- [33] K. Ward, R. Tough, and S. Watts. *Sea Clutter: Scattering, the K Distribution and Radar Performance*. The institution of Engineering and Technology, London, 2013.
- [34] Z. Yang, X. Li, H. Wang, and R. Fa. Knowledge-aided STAP with sparse-recovery by exploiting spatio-temporal sparsity. *IET Signal Processing*, 10(2):150–161, 2016.
- [35] L. Ye, Q. Yang, and W. Deng. Matrix constant false alarm rate(MCFAR) detector based on information geometry. In *2016 IEEE Information Technology, Networking, Electronic and Automation Control Conference*, pages 211–215, 2016.